JOURNAL OF OPTOELECTRONICS AND ADVANCED MATERIALS Vol. 10, No. 8, August 2008, p. 1976 - 1980

Optical diagnosis of double discharges in pulsed DBD with different barrier materials

A. S. CHIPER*, A.V. NASTUTA, G. B. RUSU, V. POHOATA, R. CAZAN, G. POPA
Plasma Physics Department, "Al. I. Cuza" University, 700506 Iasi, Romania

The experiments were performed in a double dielectric barrier discharge in He at atmospheric pressure, in glow mode of operation and presence of the secondary discharge. The study was focused on the effect of the barrier material on the characteristics of pulsed DBD. Using emission spectroscopy and tunable diode laser absorption spectrometry, complementary information on the excited species present in the discharge have been obtained. It results that the secondary discharge preserves the main characteristics of the primary one and their amplitude is dependent on the barrier material.

(Received March 1, 2008; accepted June 30, 2008)

Keywords: Atmospheric pressure glow discharge, Pulsed dielectric barrier discharge, Secondary discharge, Emission spectroscopy, Diode laser absorption spectrometry

1. Introduction

In most cases, the so called classical dielectric barrier discharge (DBD), used for applications, is driven by a sine wave voltage [1]. But, it was demonstrated that in some specific applications as ozone generation, pollutant destruction, surface treatment or excimer lamp [1-6] the pulsed DBD is more efficient than that classical one. Moreover, it was found that under some experimental conditions of pulsed barrier discharge a second current pulse with inverse polarity is induced at the decreasing applied voltage flank in addition to the main current peak [2, 3, 7, 8]. Liu and co-workers [7, 8] have shown that this secondary discharge can be produced in a large range of the gas pressure, different types of geometries and gasses, as long as unipolar square voltage pulses with fast (sub-microsecond) rising and falling flanks are applied to the reactor. However, we have also obtained the secondary discharge in impure helium and helium with reactive gasses ($He+N_2$ and $He+O_2$) in plane-parallel geometry during a semi-sine unipolar voltage pulse with slow rising and falling flank (15 μs).

In the present paper a pulsed barrier discharge in helium at atmospheric pressure, in glow mode, is discussed. The optical emission spectroscopy and tunable diode laser absorption spectrometry (TDLAS) were used to diagnose the atmospheric pressure DBD plasma in He. The study is focus on the influence of the surface properties of the barrier material on the mechanisms involved in double barrier discharges development.

2. Experimental Set-up

The experimental set-up consists of a plane-parallel geometry of DBD system (see Figure 1). The dielectrics were placed on ground electrode and high voltage electrode. The copper electrodes (5.04 cm^2 each) are centered on the dielectric plates. Two different dielectric materials have been used as barriers: ZrSnTiO ceramic (ZST) and polyethylene therephtalate (PET). The gas gap thickness was in all experiments of 3 mm. The high voltage power supply (TERAFLUX, 1 to 10 kV, pulse duration between 10 μs to 45 μs and frequency in the range 10 Hz to 10 kHz) generates monopolar semi-sine pulses. The voltage pulse with duration of 20 μs and frequency of 2 kHz were used to excite the discharge. A mass flow controller regulates the helium mass flow rate at 90 sccm. The experiments are made at room temperature, in spectral helium (Linde Gas, purity 4.6) without preliminary vacuum pumping.

The applied voltage on the electrodes, U_a, and the total current through the reactor, I, were monitorised using a 350 MHz digital oscilloscope (LeCroy WaveSurfer 434). The emission light of DBD plasma was analyzed using high resolution Triax 550 (Horiba Jobin Yvon) spectrometer with a photomultiplier and a CCD (Symphony Horiba Jobin Yvon) as detectors. The temporal variations of the spectral lines/bands emitted by DBD plasma was monitored using a photomultiplier as detector for the spectrometer.

The DL100 (TOPTICA) tunable diode laser absorption spectrometry (TDLAS) system was used. The laser was tuned around 777.194 nm wavelength, corresponding to the $3^5S_2 \rightarrow 3^5P_3$ transition of the atomic oxygen, with half-width of the laser line of about 1MHz. A 0.4 mm thick and 3 mm wide laser beam was crossing the plasma volume along to the electrodes and parallel to them, as in Fig. 1. A digital oscilloscope records the temporal evolution of the absorption signal. The absorption coefficient, k_v, was used to quantify the absorption signal as:

$$k_v=(1/L)\ln(I_o/I_v) \quad (1)$$

where: I_o and I_v are the intensity of the incident and transmitted laser beam; and L - absorbing medium path.

3. Results and Discussions

The experiments were performed in a He atmospheric pressure dielectric barrier discharge (DBD) working in glow mode, which presents two current peaks during each

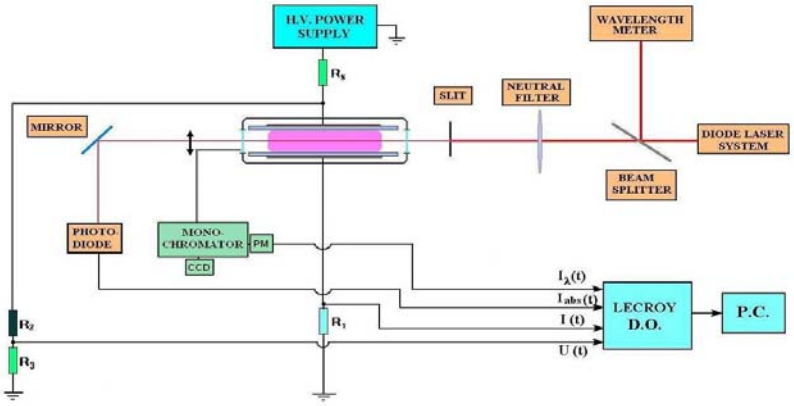

Fig. 1. The experimental set-up; R_s=7.5 KΩ, R_1=150 Ω, R_2/R_3=1000.

.

applied voltage pulse, as in Figure 2. Usually, a glow mode pulsed discharge presents only one single current peak, which corresponds to each voltage pulse. But in special experimental conditions of the pulsed barrier discharge, besides the main current pulse, a second current pulse with inverse polarity is induced at the decreasing applied voltage flank (see Figure 2). This kind of discharge is also called double discharge.

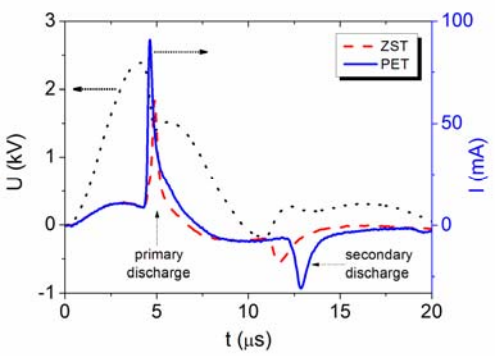

Fig. 2. Time evolution of discharge current for DBD-PET and DBD-ZST; U_a=2.5 kV=const.

The influence of the dielectric barrier material over the properties of a double pulsed dielectric barrier discharge was studied. Two different dielectric materials: ZrSnTiO ceramic (ZST) and polyethylene therephtalate (PET) were used as barriers. The parameters of the dielectrics used as barriers are given in Table 1, the thickness, d_d, the relative electrical permittivity, ε_r, the dielectric capacitance, C_d, and the equivalent electrical capacitance of the DBD system, C_{DBD} (which was calculated using equation 2). The dielectric capacitance, C_d, and the gap capacitance, C_g, were calculated taking into consideration the reactor geometry. The distance between the dielectrics being the same in all experiments, the gap capacitance was constant for both DBD systems (1.5 pF). Moreover, the gap capacitance is assumed to have the same value in presence and absence of the plasma [7]. The thickness of the dielectric plates was selected in such a way that the dielectric capacitance has approximately the same value for both types of dielectrics (see Table 1). So, the equivalent electrical capacitance of both DBD systems, C_{DBD}, has about the same value (see Table 1). In this way, the reactive effect of the capacitance on the DBD plasma properties was equivalent in both cases.

$$\frac{1}{C_{DBD}} = \frac{1}{C_d} + \frac{1}{C_g} \qquad (2)$$

Table 1. Parameters of the dielectric barriers.

Type of Dielectric Barriers	d_d *(mm)*	ε_r	C_d *(pF)*	C_{DBD} *(pF)*
PET	0.2	3	33.45	1.43
ZST	2.5	36	32.11	1.42

In spite of the fact that the electrical capacitance of the DBD system, C_{DBD}, has the same magnitude, the plasma current through DBD-PET system is significantly larger than in the DBD-ZST case, for the same value of the applied voltage (Figure 2). This result can not be explained by geometrical factor. Surface properties of the dielectric material have to be considered, while these properties may play an important role in the mechanism of the discharge by electron emission and by neutral particles desorbed or

sputtered at the surface due to ion and fast neutral bombardment. A larger electron emission at the dielectric surface may explain increasing of the discharge current for DBD-PET with respect to DBD-ZST, while the presence of impurities as oxygen, nitrogen and water molecules may change the plasma chemical reactivity in both cases. More details are given in [9].

The presence and behavior of desorbed and/or sputtered particles within the helium discharge plasma were emphasized and studied by emission and absorption spectral methods. The excited species of the He, N_2, N_2^+, OH, O^+ and O identified within the DBD emission spectrum were registered and then analyzed using a CCD camera as detector of the spectrometer (see Figure 3). Except helium atoms, as main working gas, all other particles present in the discharge are impurities desorbed or sputtered from the dielectric surfaces and walls of the discharge cell. The most intense spectral lines/bands and the corresponding energetic configurations of their transitions are presented in Table 2. The 547 nm spectral line was not investigated being a superposition of two spectral lines given by oxygen (548.10 nm) and nitrogen (546.25 nm) ion, respectively.

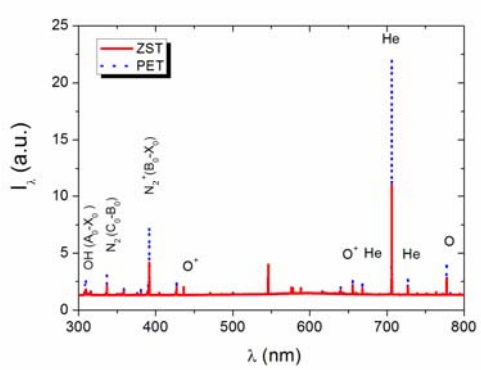

Fig. 3. Comparison between emission spectrum of DBD plasma with different dielectrics: ZST ceramic and PET, U_a=2.5 kV=const.

Table 2. Selected spectral transitions.

Species	*Transitions*	*λ (nm)*	*$E_{threshold}$ (eV)*
N_2	$C\ ^3\Pi_u \rightarrow B\ ^3\Pi_g$,	337.1	11.03
O	$3p\ ^5P^0_2 \rightarrow 3s\ ^5S^0_2\ ^5S^0_2$	777.4	10.74
N_2^+	$B\ ^2\Sigma_u^+ \rightarrow X\ ^2\Sigma_g^+$	391.5	18.75
He	$3s\ ^3S \rightarrow 2p\ ^3P$	706.5	22.72
He	$3d\ ^1D \rightarrow 2p\ ^1P$	667.8	23.16
He	$3s\ ^1S \rightarrow 2p\ ^1P$	728.1	22.92
O^+	$4p\ ^2D \rightarrow 35\ ^4D$	655.0	30.75

The experimental result presented in Figure 3 shows increasing of the spectral lines intensity for DBD-PET system, which correspond to increasing of the discharge current presented in Figure 2.

Relevant information concerning the role of elementary processes within plasma volume is obtained from time variation of the spectral lines/bands intensities. The variation of the maximum spectral line intensity was measured, using photomultiplier as detector and presented comparatively with temporal evolution of the discharge current. There are two groups of spectral lines. One group consists of He spectral lines, of which time variation of light intensity is in phase with time variation of the discharge current (Figure 4). The second group consists of O, O^+ spectral lines and N_2, N_2^+ and OH bands, of which time variation of light intensity are delayed with respect to time variation of the discharge current (Figure 5).

These results can be explained taking into account the main elementary processes, as collisions, within the plasma volume. The elastic collisions play the main role in diffusion process and mobility of the particles. But, inelastic collisions will be in the following considered because these elementary processes may explain plasma production and may influence directly plasma reactivity and processes at plasma surface interaction. There are two main elementary processes, as inelastic collisions. One is related to electron-neutral collision and the second one to neutral-neutral and/or ion-neutral collision.

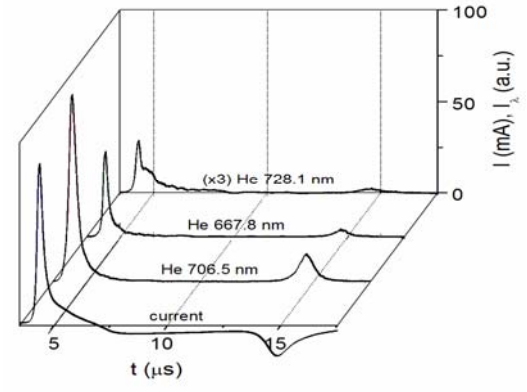

Fig. 4. Time evolution of He spectral lines and discharge current.

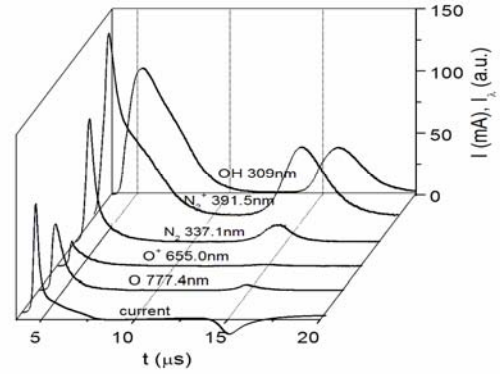

Fig. 5. Time evolution of the O and O^+ lines and N_2, N_2^+ and OH bands.

The structure of the helium atom is a very special one with the highest energy of ionisation among all elements, (24.588 eV) and also highest energy of the first excited states (20.61 eV for 1s2s ^{1}S and 19.82 eV for 1s2s ^{3}S). Moreover, both first excited states are metastable ones with rather long lifetime (2 microseconds). Consequently, in helium discharges the energetic electrons have to play essential role first in ionisation process and plasma

generation with an important population of metastable atoms with high energetic state. It implies the fact that helium discharges must have an important group of energetic electrons able to sustain the process of plasma generation but they may also excite helium atoms.

In glow mode discharge the fast electrons may originate within cathode fall region [10]. At atmospheric pressure the ionization collision frequency of the 100 eV electrons in helium is $5.10^{11}s^{-1}$ (transition He $1s^2\ ^1S \rightarrow He^+$ 1s) [11], while the excitation collision frequencies for helium excited states: 3s ^{1}S, 3s ^{3}S and 3s ^{1}D, presented in Table 2, are about one order of magnitude lower. Moreover, the life time of these excited states is 55 ns, 65 ns and 15 ns, respectively, which is shorter or comparable with characteristic time (about 100 ns) of the discharge current, defined as time interval in which amplitude of the discharge current peak decreases of factor *e*. Consequently, intensities of the helium spectral lines (677.8 nm, 706.5 nm and 728.1 nm) will follow time variation of the discharge current as it is presented in Figure 4.

The electron collision frequencies for helium atom excitation on the metastable state (^{1}S and ^{3}S, respectively) are 1.6 and $0.6x10^{10}$ s^{-1} [11]. This fact shows that within helium discharge plasma the energetic electrons may produce, besides ionisation, a fraction of metastable atoms, which play an important role in the balance of the neutral-neutral collisions with atoms and molecules of oxygen and nitrogen impurities as the reactions 3 to 5:

$$He^m + N_2 \rightarrow He + N_2^+(B) + e \quad (3)$$

$$He^m + O_2 \rightarrow He + (O_2^+)^* + e \quad (4)$$

$$(O_2^+)^* + e \rightarrow O^* + O \quad (5)$$

Therefore, excitation mechanism for the O, O^+ spectral lines and N_2, N_2^+ and OH bands is different then that of helium atoms. So, due to the fact that N_2^+ excited species were identified in emission spectrum, we have presumed that the Penning ionisation of nitrogen molecules via helium metastable atoms (reaction 3) is a possible mechanism for ionisation and excitation of the nitrogen. In order to confirm this mechanism, temporal evolution of the spectral lines/bands was registered. Figure 5 clearly shows delay of the N_2^+ excited species against discharge current and a longer duration of light emission, which correspond to longer helium metastable life time.

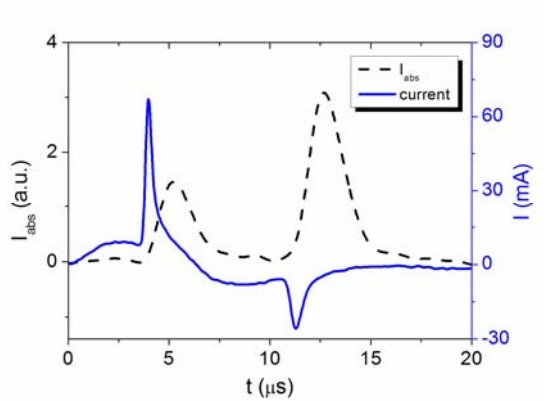

Fig. 6. Time evolution of discharge current and absorption intensity oxygen atoms at 777.194 nm, for DBD-ZST

Moreover, the atomic oxygen responsible for 777.4 nm spectral line could be produce by chain reactions (4) and (5) [12]. This is also proved in Figure 5, which emphasizes that the O excited species are delayed against the discharge current. So, we can conclude that the oxygen species are also excited in stepwise process, including helium metastables, which are produced by direct electron neutral collision.

Complementary information on the excited species present in the discharge was obtained using tunable diode laser absorption spectrometry technique, besides those obtained by optical emission spectroscopy. The absorption signal of oxygen metastables from the DBD system was recorded, for different types of dielectric barriers, but for the same value of the applied voltage. For both dielectric materials, time evolution of the absorption signal clearly shows same order of magnitude (μs) of the delay of the atomic oxygen line of 777.194 nm with respect to both primary and secondary discharge (Figure 6).

4. Conclusions

By using two distinct techniques, the emission spectroscopy and tunable diode laser absorption spectrometry, we have obtained complementary information on the excited species present in a double discharge with two different types of dielectric barriers: ZST ceramic and PET. It results that both pimary and secondary discharge has relatively the same mechanism of excitation.

Concluding, the secondary discharge preserves the main characteristics of the primary one and their amplitude is dependent on the barrier material. A larger electron emission at the dielectric surface was assumed to cause this dependence.

Acknowledgement

Romanian Ministry of Education and Research supported this work under grant CNCSIS type AT no. 159/2007.

References

[1] U. Kogelschatz, Plasma Chemistry and Plasma Processing, **23**(1), 1, (2003).
[2] S. Liu and M. Neiger, Proc. of the 13th Int. Conf. on Gas Discharges and their Applications, Glasgow, Great Britain, 3-8 September, 1, 263 (2000).
[3] M. Laroussi, X. Lu, Journal of Applied Physics, **96**(5), 3028 (2004).
[4] X.Pei, M. Laroussi, J. Phys. D: Appl. Phys., **39**, 1127 (2006).
[5] K. Okazaki, T. Nozaki, Pure Appl. Chem., **74**(3), 447 (2002).
[6] F. Vollkommer, L. Hitzschke, Proc. 8. th. Int. Symp. Sci. Tech. Light Sources, Greifswald, Germany, 51, August 1998.
[7] S. Liu, M. Neiger, J. Phys. D: Appl. Phys. **34**, 1632 (2001).
[8] S. Liu and M. Neiger, J. Phys. D: Appl. Phys. **36**, 1565 (2003).
[9] A. S. Chiper, A. Nastuta, G. Rusu, G. Popa, Journal Optoelectron. Adv. Mater. **9**(9), 2926 (2007).
[10] Tochikubo, F., Chiba, T. and Watanabe, T., Jpn J. Appl. Phys., **3**, 5244, 1999.
[11] R.K. Janev, W.D. Langer, K. Evans, Jr., D.E. Post, Jr. Elementary processes in Hydrogen-Helium Plasmas, Springer-Verlag Berlin Heidelberg 1987.
[12] W. P. West, T. B. Cook, F. B. Dunning, R. D. Rundel R. F. Stebbings, J. Chem.Phys. **63,** 1237 (1975).

*Corresponding author: alina.chiper@uaic.ro